Proceedings of the Indian National Science Academy (2025) 91:783–803
https://doi.org/10.1007/s43538-024-00357-z

RESEARCH PAPER

Characterizing temporal variability in meteorological parameters patterns in the Asan River Watershed, Uttarakhand, India: insights from long-term data analysis

Ankita Sharma[1] · Radha Krishan[2] · Bhaskar Nikam[3] · Dhirendra Singh Bagri[4]

Received: 10 April 2024 / Accepted: 1 October 2024 / Published online: 17 October 2024

Abstract
Assessing fluctuations in meteorological parameters such as rainfall and temperature often entails identifying and characterizing trends and variations, particularly in regions where rainfed agriculture predominates. In this study, gridded datasets of rainfall and temperature were utilized to analyse trend detection and variability patterns in the Asan River watershed, situated in Doon Valley, Uttarakhand, India. These datasets, obtained from the Indian Meteorological Department (IMD) portal, had spatial resolutions of $0.25° \times 0.25°$ and $1° \times 1°$ for rainfall and temperature, respectively. The gridded datasets were subjected to analysis to identify time series trends utilizing methods such as the Mann–Kendall test, coefficient of variation, Sen slope estimator, and anomaly index. The study encompasses the integration, processing, and evaluation of these datasets spanning approximately four decades to explore changes in monthly and annual maximum, minimum, and mean values, aiming to uncover potential variations in rainfall and temperature within the region. The comprehensive analysis unveiled a sustained long-term increase in annual rainfall within the watershed. Noticeable fluctuations in rainfall trends were observed, with the rainfall anomaly analysis revealing an equal distribution of 23 years categorized as rainy and dry seasons, respectively. Similarly, the regression analysis of annual mean temperature also indicated statistically significant positive trends. Furthermore, the analysis of long-range temperature anomalies in mean annual temperature demonstrated inter-annual variability, with a consistent upward trend observed from 1997 to 2013. Recommendations are crucial to devising strategies in the agricultural sector, which must consider the declining and erratic nature of rainfall and the increasing trend of temperature.

Keywords Meteorological parameters · Trend detection · Variability patterns · MAKESENS · Mann–Kendall test · Coefficient of variation · Sen slope estimator · Anomaly index · Climate change

Introduction

Climate is defined as “the fusion of different weather elements widespread over 30 years” (Ayoade 1983). These elements include temperature, precipitation, wind, relative humidity and pressure, among others (Rao et al. 2007). The variation of climate and temperature in our globe is due to the rise in the concentration of Green House Gases and Carbon Dioxide in the atmosphere. The small sustainable farms especially those that are strongly dependent on rainfed agriculture are severely affected by rainfall variability. Weather elements like precipitation and temperature are significant variables in climatic sciences and hydrology. These elements are used frequently to trace the magnitude and extent of climatic change and variability (Parry et al. 2007). Climate plays a significant part in shaping hydrology and water quality. Over a decade several researchers confirmed that because of industrialization and urbanization, the global surface temperature has been soaring (Karl et al. 1993). Previous studies also suggest that several anthropogenic factors viz., increase in emission from vehicles, land use/land cover changes, deforestation, draining of wetlands, and industries, lead to alter the albedo of the atmosphere and

✉ Ankita Sharma
ankita.geors@gmail.com

[1] Department of Geology, HNBGU, Srinagar, Uttarakhand 246174, India

[2] Department of Civil Engineering, Government Engineering College, Banka, Bihar 813102, India

[3] EDPO, ISRO, Bangalore, Karnataka 560096, India

[4] Department of Geology, S.R.T. Campus, HNBGU, New Tehri, Uttarakhand 249001, India

contribute to increasing diurnal temperature variation (Tigga and Hema Malini 2011). Such activities further influence the variability of weather elements (Landsberg 1984). There is a strong need to study the spatiotemporal dynamics of meteorological variables, especially about climate change with great emphasis given to rainfed agriculture. UAPCC (2014) also emphasized the potential effect of climate change especially on small farmers as they are mostly dependent on traditional methods of crop cultivation. Rainfall and temperature affect climate variability to a major extent to determine the cultivation of the crop in different parts of the globe. Climate change and variability have been discussed by various researchers which include the following: Pandey and Ramasastri (2001), Hamilton et al. (2001), Birsan et al. (2005a, b), Modarres and Silva (2007), Longobardi and Villani (2010), Kumar et al. (2010), Jhajharia et al. (2015, 2009, 20122014), Gajbhiye et al. (2016a, b), Krishan et al. (2016), Asfaw et al. (2018), Ademe et al. (2020) and others.

The trend detection of discharge, runoff and precipitation, gives necessary information regarding future possibilities of planning, development and management of water resources in the region (Hamilton et al. 2001; Yue and Wang 2004). Trend and variability analysis of rainfall are the most significant aspects in the studies of climate change. The variation in rainfall patterns, floods due to heavy rainfall and the severity of drought conditions affect the hydrological, agricultural and economic status of the country. India faces a series of disasters because of changes in climatic conditions. Uttarakhand has been experiencing tremendous changes in its climate over the last several decades (Singh et al. 2013).

The temperature rise is associated with global climate change. Urbanisation and the creation of cities into industries and factories affect the temperature and rainfall on a decadal scale. The uneven distribution of rainfall and rising temperature is the major concern in the area (Sharma et al. 2021). In our previous study on urban sprawl expansion in the area (Sharma and Bagri 2020), we concluded that over the last 40 years (1980–2016), the land use and land cover (LULC) patterns have undergone significant changes, with settlement increasing fourfold. In the area shows significant changes and the settlement increased by four folds. The manifold increase in the population, habitation and so the number of vehicles are the prime factors responsible for changing weather and ultimately climatic patterns. This effect of changing climate has direct impacts on atmospheric conditions, water resources and natural systems (Singh et al. 2013; CCSP 2014; UAPCC 2014).

In this research, the evaluation of changing long-term trend variation of meteorological variables such as rainfall and temperature for the past 46 and 39 years respectively in the Asan watershed and its surroundings is done. The gridded dataset of the used climatic parameters is obtained from the Indian Meteorological Department (IMD) portal. In a larger watershed (> 100 km^2), the spatial variability of precipitation becomes significant (Negi 2002). The study area has experienced severe variation in its climate for the last several decades. Due to urbanization and an increase in temperature, the variability of weather and climate patterns of the Doon Valley is severely affected (Sharma et al. 2024). An increase in temperature leads to an increase in weather variability. As an outcome, meteorological data must be observed, monitored and analysed. The prime objective of this study is mentioned below:

- Preparing and analysing the changing long-term trend series of rainfall and temperature gridded datasets using the trend detection method.
- To examine the spatial and temporal variability, magnitude and coefficient of variance of both the datasets.
- To examine the anomaly index to determine the most extreme phases over the study period.

Study area

The Asan River watershed is situated between geographic latitudes 30°14′14″ N to 30°29′54″ N and longitudes 77°39′42″ E to 78°05′30″ E in the Dehradun district of Uttarakhand State, India. It spans an elevation range from 345 to 2188 m above mean sea level (MSL) and covers an area of approximately 712.34 km^2 (Fig. 1). The watershed falls within the 53F/11, 53F/15, 53J/3, and 53F/16 toposheets of the Survey of India, with a scale of 1: 50,000. Positioned in the Doon valley at the foothills of the Siwalik ranges, the Asan River flows centrally through the valley from northeast to southwest. Stretching approximately 40 km in length and with an approximate width of 18 km, it holds significant importance in the region. The climate of the watershed varies depending on its elevation, ranging from tropical to cold and rainy. The surrounding hilly terrain contributes to significant temperature fluctuations due to elevation differences (Sharma et al. 2020). The Siwalik hills, with an elevation of about 800 m, experience a sub-tropical climate, while areas with elevations ranging from 800 to 2400 m have a temperate climate (Chauhan 2010). The physiography of the watershed is characterized by the abrupt rise of the Lesser Himalayan range (Mussoorie Hill) in the north and the Siwalik range in the south. Due to its physiography, the movement of monsoon winds in the watershed is significantly impeded, resulting in rainfall. Summer rainfall constitutes approximately 85% of the total annual rainfall, playing a crucial role in replenishing water resources. While summers are pleasant in the hilly regions, they do not offer the same relief as in the adjacent plains. On average, the area receives 1499.2 mm/

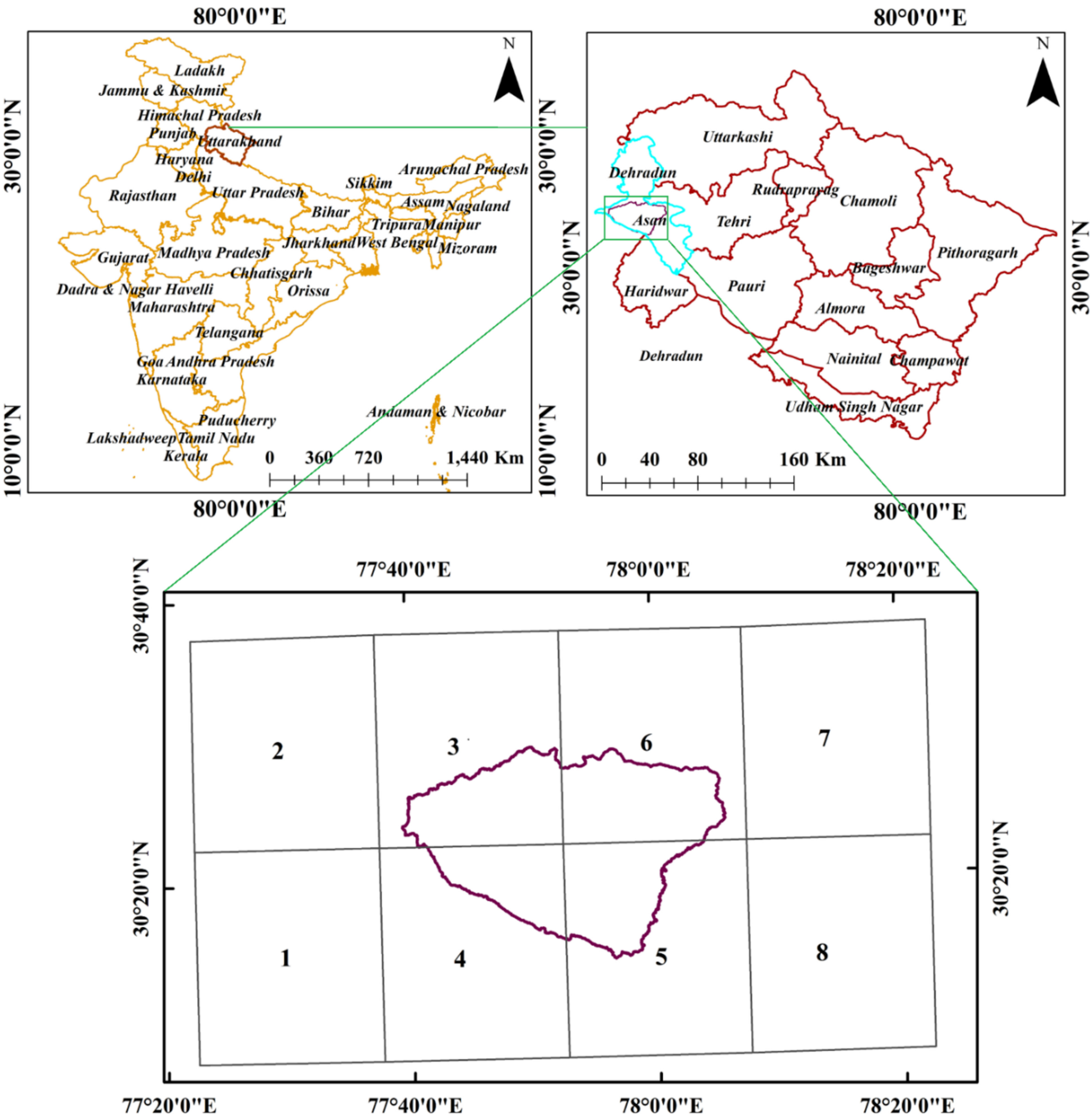

Fig. 1 Location of the study area; Distribution of grids covering the watershed's boundary and the surrounding region

year of annual rainfall, with the majority occurring from June to September, and July and August being the wettest months. Rainfall plays a vital role in the rainfall-runoff relationship, with the Song-Suswa river system draining heavy rainfall eastwards and being joined by significant Himalayan streams such as Rispana, Bindal, Asan, Tons, Sitala, and Suarna, among others. This research focuses on studying the watershed and its surrounding areas, which are situated within 8 grids utilized for the study. Figure 1 depicts the geographic location of the watershed within grids.

Methodology and data used

The daily gridded rainfall data with a resolution of 0.25° × 0.25° for the last 46 years (1970–2015) and temperature data having a spatial resolution of 1° × 1° for the last 39 years (1975–2013) are studied here to achieve the objective. To examine the temporal and spatial variability of the study area, these gridded datasets of rainfall and temperature have been obtained from the Indian Meteorological Department (IMD) portal. To ascertain the trend and magnitude of slope in the rainfall and temperature datasets within the study area, we employed an Excel macro template called MAKESENS, developed by Salmi et al. (2002). This template incorporates the conventional Mann–Kendall (MK) test proposed by Mann (1945) and Kendall (1948) for detecting trends, as well as Sen's Slope Estimator proposed by Sen (1968) for estimating slope magnitude. These analyses were conducted after eliminating any significant autocorrelation coefficient effects. These non-parametric methods are widely used for analysing the trends in several hydrological uses viz., rainfall, temperature, evapotranspiration, wind speed etc. (Jhajharia et al. 2009, 2012, 2014, 2015).

Statistical test for rainfall trend detection methods

Statistical determination of variation in a random variable is commonly achieved through trend detection methods (Haan 1977). These methods typically employ either parametric or non-parametric tests to assess the significance of trends. Trend-based analysis relies on time series data of annual and seasonal weather elements. The key steps involved in this analysis include: (a) assessing correlation effects, (b) detecting trends using the MK-test, and (c) estimating trend magnitude using Sen's estimator. Non-parametric trend detection methods are specifically applied to persistent datasets. The MK-test, a widely used non-parametric test for trend detection in meteorological variables, is particularly suitable for datasets with unusual dispersion and unaccounted data points in the time series (Degefu and Bewket 2014; Tabari et al. 2015; Kiros et al. 2016). This test aids in identifying monotonic trends and determining their statistical significance in climatic, meteorological, and environmental datasets (Yue et al. 2002). Due to deviations present in some datasets, the Mann–Kendall test is preferred because it is based on the presence of positive or negative signs, making trend determination less susceptible to these deviations (Birsan et al. 2005a, b). The formula for the Kendall test statistic represented by '*S*' of the series '*x*' is given by Mann (1945), Kendall (1948) and Yue et al. 2002 [Eq. (1)]:

$$\boldsymbol{S} = \sum_{i=1}^{n-1} \sum_{j=i+1}^{n} \boldsymbol{sgn}\left(\boldsymbol{x}_j - \boldsymbol{x}_i\right) \tag{1}$$

where 'x_i' and 'x_j' are the time series which is ranked from $i = 1,2, \ldots, n-2$ and $j = i+1,2,\ldots,n$ respectively; the signum function is denoted by '*sgn*'; the sample size is denoted by '*n*'. The variance in association with '*S*' is denoted as '$V(S)$' and adopted from Mann (1945) and Modarres and Silva (2007), is calculated using the given formula [Eq. (2)]:

$$\boldsymbol{V}(\boldsymbol{S}) = \frac{\boldsymbol{n}(\boldsymbol{n}-1)(2\boldsymbol{n}+5) - \sum_{m=1}^{p} \boldsymbol{ty}(\boldsymbol{ty}-1)(2\boldsymbol{ty}+5)}{18} \tag{2}$$

where '*p*' is the number of tied groups; '*ty*' is the number of data points in group '*y*'; 'n' is the number of observations, in a case where the sample size $n > 10$, the '*Zc*' test statistics are calculated using this formula [Eq. (3)]:

$$\boldsymbol{Zc} = \begin{cases} \frac{S-1}{\sqrt{V(S)}}, & \text{if } S > 0 \\ 0 & \text{if } S = 0 \\ \frac{S+1}{\sqrt{V(S)}}, & if\, S < 0 \end{cases} \tag{3}$$

The negative '*Zc*' depicts decreasing (downward) trends which represent the cooling phase whereas the positive '*Zc*' depicts increasing (upward) trends representing the warming phase for the particular period. The '*Zc-statistics*' obeys normal distribution. When the '*Zc*-statistics' is more than the quality deviation of '$Z_{1-\alpha/2}$' for the accepted value of '*α*', (α is the significance level which indicates the strength of the trend), is considered to be statistically significant. In the present study, the significance level of $\alpha \leq 0$ is established for the evaluation of trends.

Magnitude of the trend

Singh (2012) in his book "*Global Warming: Impacts and Future Perspective*" describes the estimation of slope and intercept which is further initiated as Sen's slope test. Theil (1950) and Sen (1968) predicted the magnitude of the trend series. In the present study, the method adopted from the Theil-Sen approach and Sen's slope estimation method is used to analyse the significant linear trend and evaluate the true slope of the linear trend respectively. To evaluate the true slope of an existing trend '$\boldsymbol{f(t)}$', Sens's slope estimation method is used [Eq. (4)], where the trend is supposed to be linear such as:

$$\boldsymbol{f}(\boldsymbol{t}) = \boldsymbol{Qt} + \boldsymbol{B} \tag{4}$$

where '*Q*' is the slope, '*B*' is the constant intercept and '*t*' is time. In general, the slope '*Q*' between data value pairs of a time series '*x*' is estimated using the formula [Eq. (5)]:

$$\boldsymbol{Q} = \frac{\boldsymbol{x}_m - \boldsymbol{x}_n}{\boldsymbol{m} - \boldsymbol{n}}, \quad \boldsymbol{n} \neq \boldsymbol{m} \tag{5}$$

where 'x_m' and 'x_n' are the data value pairs at time '*m*' and '*n*' (m > n) correspondingly.

The median for a time series '*x*' having '*n*' observation, the '*Q*' can be evaluated as $N = n(n-1)/2$ values. In the mentioned procedure '*N*' value of '*Q*' is ranked from minimum to maximum and the Sen's estimator reads. Sen's estimator method suggests, that the overall estimator of slope

'Q^*' is the median of these 'N' values of 'Q' and is depicted by the following formula (Eq. 6):

$$Q* = \begin{cases} Q_{(N+1)/2} & \text{if } N \text{ is odd} \\ \frac{Q_{N/2}+Q_{(N+2)/2}}{2} & \text{if } N \text{ is even} \end{cases} \tag{6}$$

In the time series estimation, positive and negative values of 'Q^*' are associated with upward/increasing and decreasing/downward trends respectively.

Coefficient of variation:

The analysis of rainfall variability is measured by the Coefficient of Variation (CV). A lower value of 'CV' is the indicator of less variability of rainfall and vice versa (Gajbhiye et al. 2016a, b) which is computed as [Eq. (7)]:

$$\boldsymbol{CV = \frac{\sigma}{\mu} \times 10} \tag{7}$$

where 'CV' is the Coefficient of Variation, 'σ' is a standard deviation and 'μ' is mean precipitation. According to Hare's classification (2003), which is based on the degree of rainfall variability events is less (CV < 20), moderate (CV = 20–30), and high (CV > 30).

Rainfall trend analysis

To assess monthly and annual variations in rainfall series and identify the driest and wettest months and years, two approaches are employed: (1) Analysis based on average annual and seasonal rainfall gridded datasets, where trend analysis is conducted using the Mann–Kendall test and Sen's Slope estimator (2) Identification of the driest and wettest months through the rainfall anomaly index. The seasonal distribution of months for the rainfall data is categorized as follows:

i. December to February (winter).
ii. March to June (summer).
iii. July to September (monsoon).
iv. October to November (post-monsoon).

Statistical characteristics of annual and seasonal rainfall based on the gridded dataset

Precipitation is a significant meteorological parameter, which directly affects the productivity of crops and relative aspects of water resources and availability. The analysis of mean, standard deviation and coefficient of variation for a basic grid-based statistical parameter of seasonal and annual rainfall episodes for 46 years (1970–2015) is evaluated in this study. The seasonal rainfall episodes include monsoon, post-monsoon, summer and winter. Table 1 shows the preliminary grid-based statistics of annual and seasonal mean rainfall data in the watershed. The annual mean rainfall across all grids ranges from 1274.0 to 1766.9 mm/year, with a weighted average rainfall of 1498.58 mm/year. Figure 2a–e illustrates the grid-based graphical representation. In the case of the monsoonal episode, mean values range from 645.10 to 1075.9 mm/year across all grids with the weighted average rainfall of 854.75 mm/year. In post-monsoon, values range from 23.8 to 37.9 mm/year within grids with a weighted average rainfall of 31.5 mm/year. Winter rainfall varies from 235.6 to 338.5 mm/year across all grids with a weighted average rainfall of 291.98 mm/year. In summer, the mean value ranges from 95.9 mm/year to 148.1 mm/year across all grids with a weighted average rainfall of 115.8 mm/year. These findings suggest that the areas with lower rainfall have more variability compared to those with higher rainfall (Gajbhiye et al. 2016a, b). The observation of annual and seasonal rainfall indicates that the year 1976 is considered the driest, with a minimum rainfall of 918.0 mm/year, while 2010 is the wettest with a maximum of 2352.9 mm/year.

Table 1 Statistics of grid-wise mean annual and seasonal rainfall in the area

Grid	Annual rainfall (mm)	Monsoon rainfall (mm)	Post-monsoon rainfall (mm)	Summer rainfall (mm)	Winter rainfall (mm)
1	1310.4	774.6	26.5	235.6	95.9
2	1504.8	910.4	29.5	280.0	106.6
3	1590.5	897.9	37.9	307.9	128.0
4	1766.9	1075.9	34.1	301.7	104.1
5	1627.7	987.2	28.9	279.9	96.0
6	1556.2	863.8	34.5	326.8	131.4
7	1358.2	645.1	37.2	338.5	148.1
8	1274.0	683.1	23.8	265.5	116.7

Analysis of *Zc*-statistics of seasonal and annual rainfall trends

Table 2 displays the *Zc*-statistics of the monthly rainfall time series spanning from 1970 to 2015. Monsoon dominates the watershed, with maximum annual average rainfall, predominantly in July, August and September. Figure 2a–e depicts annual and seasonal rainfall trends. The *Zc*-statistics revealed that both annual and monsoonal rainfall exhibits an upward trend, except for grids 6 and 8, which display an insignificant decreasing trend. In the annual time series, grid 2 demonstrates a significance

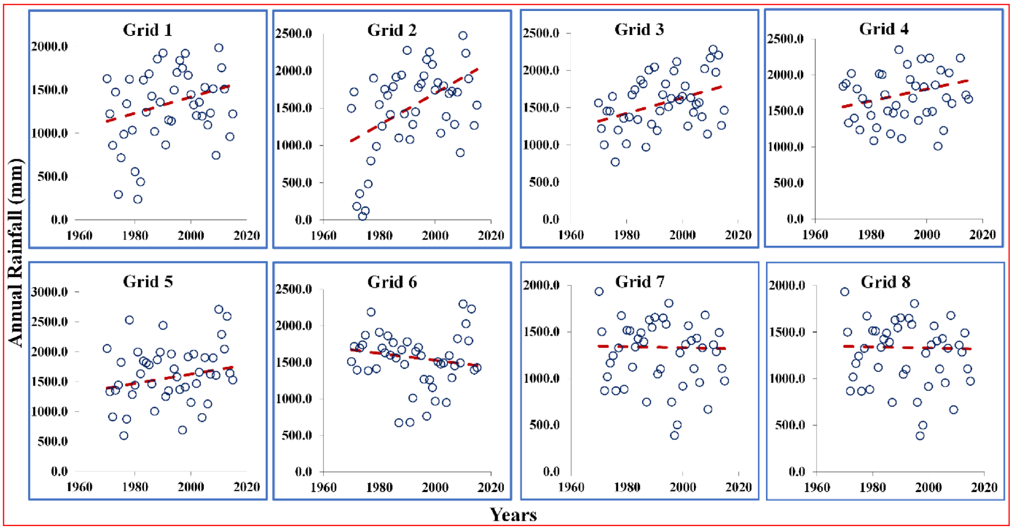

(a): Grid-based annual rainfall trend

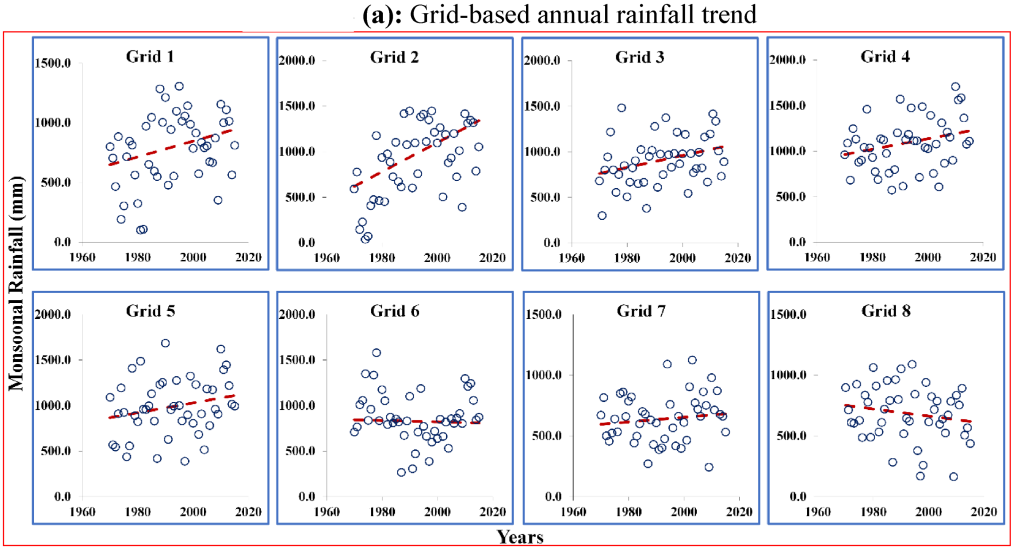

(b): Grid-based monsoonal rainfall trend

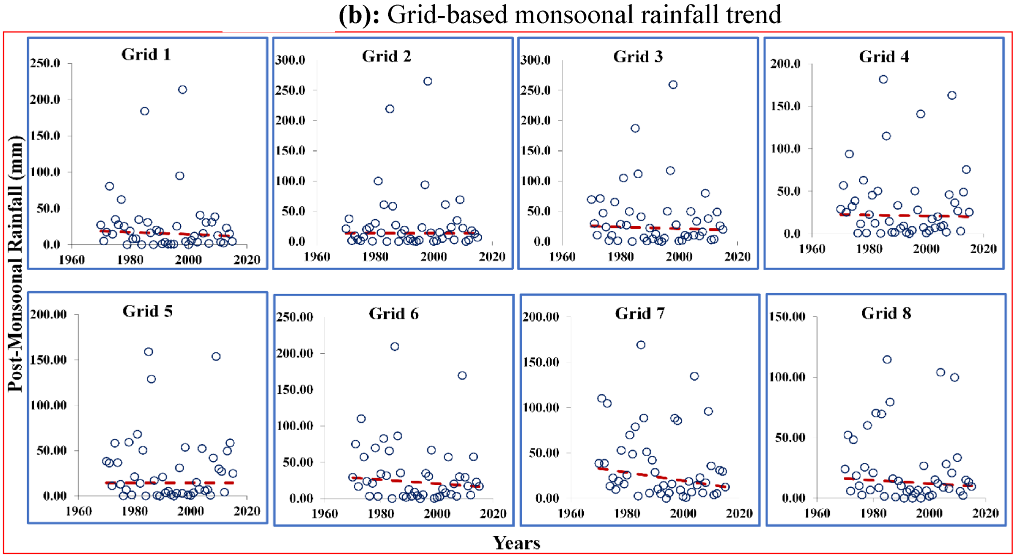

(c): Grid-based post-monsoonal rainfall trend

Fig. 2 **a** Grid-based annual rainfall trend. **b** Grid-based monsoonal rainfall trend. **c** Grid-based post-monsoonal rainfall trend. **d** Grid-based summer rainfall trend. **e** Grid-based winter rainfall trend

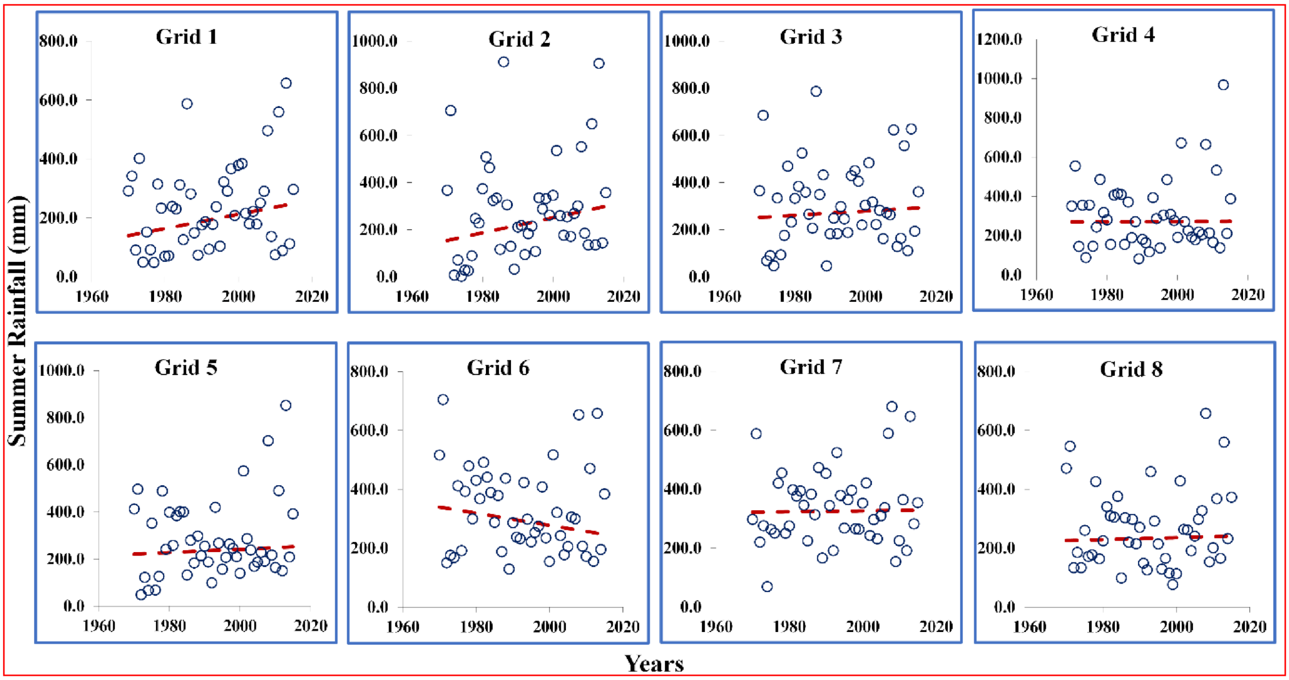

(d): Grid-based summer rainfall trend

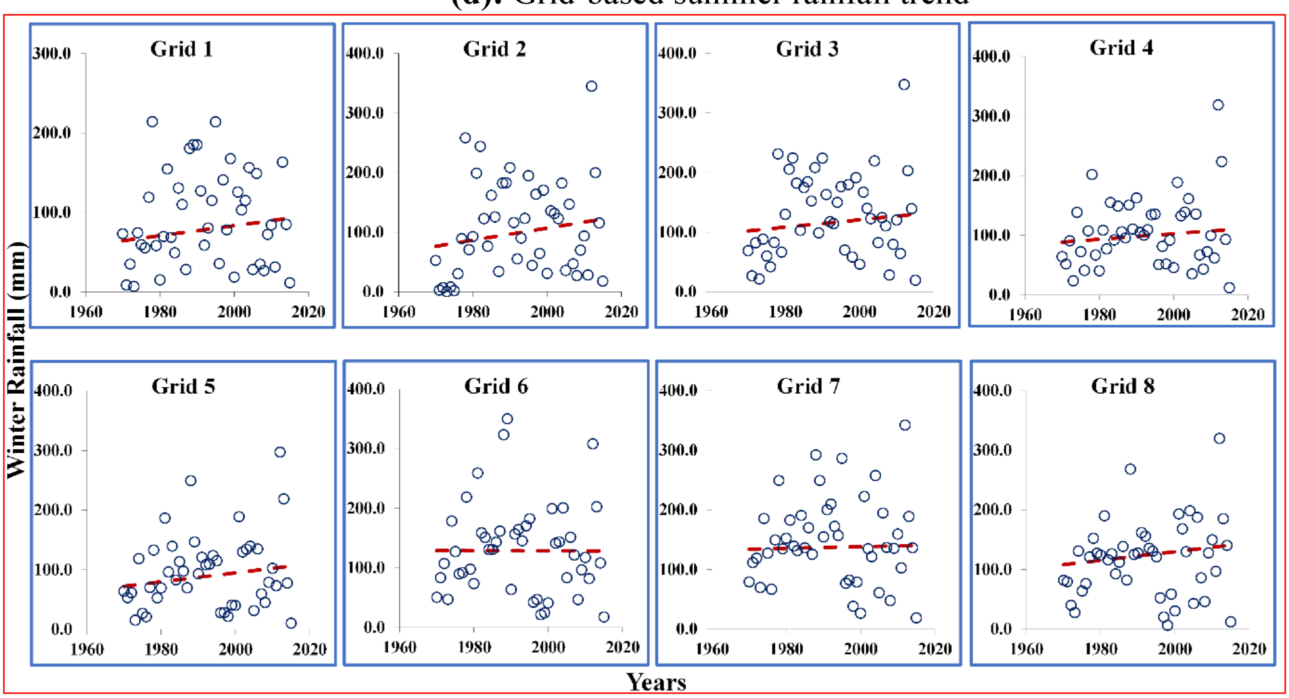

(e): Grid-based winter rainfall trend

Fig. 2 (continued)

level of 1%, while grid 3 shows 5%, and grids 1 and 4 show 10%. Similarly, in the monsoonal time series, grid 2 shows a significance level of 1%, grid 3 shows 5%, and grids 1 and 4 show 10%. Grid 8 exhibits a decreasing trend for annual, monsoon and post-monsoon rainfall while showing an increasing trend for summer and winter. This suggests that decreased rainfall may result in increased rainfall amounts during the summer and winter seasons. In the post-monsoon time series, all grids show insignificant decreasing trends except for grid 7, which demonstrates a significant decreasing one. Grid 5 of the same time series shows no variation in trend, possibly due to

Table 2 Representation of *Zc*-statistics for the annual and seasonal rainfall

Grid	Annual	Monsoonal	Post-monsoonal	Summer	Winter
1	**1.86**[c]	**1.89**[c]	− 0.89	1.48	0.91
2	**2.99**[b]	**3.39**[b]	− 0.08	1.51	1.19
3	**2.10**[a]	**2.23**[a]	− 0.71	0.38	0.55
4	**1.70**[c]	**1.76**[c]	− 0.21	0.00	0.62
5	1.55	1.55	0.00	0.34	1.17
6	− 1.04	− 0.34	− 1.04	− 0.98	− 0.02
7	0.89	0.83	**− 1.72**[c]	0.13	0.19
8	− 0.09	− 1.2	− 0.86	0.17	1.31
Mean	**1.97**[c]	2.31	− 0.64	0.21	0.64

Numbers in bold indicate significant values

[a]Significant at the 5% level

[b]Significant at the 1% level

[c]Significant at the 10% level

depletion of water availability over time. The decreasing trend in post-monsoon rainfall series has led to a decrease in their amounts during the non-monsoon period, potentially resulting in reduced runoff from the area. In terms of seasonal time scale, the summer and winter time series across all grids display an insignificant increasing trend, with grid 6 exhibiting a negative one. Figure 3 illustrates that the number of positive trends in the rainfall series is higher than the negative ones.

Analysis of seasonal and annual variability pattern of rainfall

The variability of annual and seasonal rainfall in the study area has been evaluated using the Coefficient of Variance (CV) for the time series. It statistically measures the deviation of specific data points from their mean value. Table 3 illustrates that seasonal rainfall variation is higher than annual variation. The 'CV' of mean annual and monsoonal rainfall for the study area ranges from 23.94 to 39.64% and 26.16 to 43.9% respectively, with the weighted mean of 29.04 and 33.08%, respectively. For the post-monsoon rainfall time series, the 'CV' percentage ranges from 105.27 to 174.47%, with the weighted mean for all grids of 134.13%. Mean summer and winter rainfall exhibits 'CV' percentages range from 37.5 to 74.98% and 47.95 to 73.22%, respectively, with weighted means for all grids of 54.74 and 59.31%. These statistics indicate that areas with lower rainfall experience greater variability than regions with

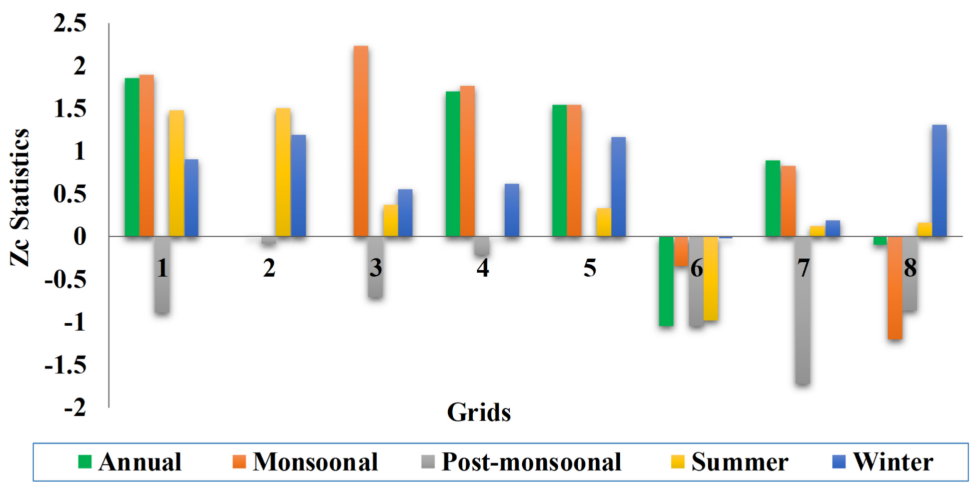

Fig. 3 *Zc*-statistics for the annual and seasonal rainfall

Table 3 Grid-wise statistics of Coefficient of Variance (CV) in percentage

Grid	Mean annual	Mean monsoon	Mean post-monsoon	Mean summer	Mean winter
1	33.50	39.55	158.79	61.16	68.18
2	39.64	43.90	174.47	74.98	73.22
3	23.94	29.46	132.78	55.42	53.93
4	25.17	26.16	124.68	57.49	54.85
5	29.30	31.53	129.36	58.38	63.97
6	25.82	31.17	124.58	43.78	58.08
7	26.69	30.26	105.27	37.50	47.95
8	28.30	32.62	123.14	49.23	54.32

relatively higher ones. Grid 2 shows the maximum values of annual and seasonal rainfall variability. Each grid of annual and seasonal rainfall has a lower value of 'CV', suggesting comparatively higher rainfall in those areas.

Rainfall variation is a common characteristic of the dataset and underscores the importance of understanding water requirements for irrigation purposes. The prevalence of lower CV values in most pixels indicates higher inter-annual variability of post-monsoon rainfall compared to annual rainfall. According to Pandey and Ramasastri (2001) and Turkes (1996), areas with higher inter-annual variability are more susceptible to floods and drought.

Magnitude of rainfall series

Table 4 displays the magnitude of the annual and monsoonal rainfall series, ranging from − 0.60 at grid 8 to 21.3 at grid 2, and from − 0.77 at grid 6 to 16.1 at grid 2, respectively. As depicted in Fig. 4, rainfall trends exhibit significant variations in magnitude and direction across different grids. Grids 6 and 8 display a negative (decreasing) trend for both annual and monsoonal time series. In the post-monsoon period, all values indicate a negative (decreasing) trend, except for grid 5, which shows no discernible trend. Conversely, for the summer and winter seasons, all grids exhibit a positive (increasing) trend, except for grid 6 of Sen's estimator. The results are quite significant, as similar grids observed statistically positive and negative slopes and trends for different time series (Tables 2, 3).

Table 4 Sen's slope values for the annual and seasonal rainfall

Grid	Annual	Monsoonal	Post-monsoonal	Summer	Winter
1	9.32	6.57	− 0.145	2.42	0.63
2	21.3	16.1	− 0.008	3.22	1.10
3	10.5	6.58	− 0.141	0.89	0.62
4	8.2	5.76	− 0.054	0.06	0.47
5	7.79	5.4	0.00	0.67	0.76
6	− 4.74	− 0.77	− 0.27	− 2.05	− 0.02
7	4.38	1.92	− 0.45	0.144	0.14
8	− 0.60	− 2.94	− 0.13	0.32	0.73
Mean	7.89	4.96	− 0.16	0.23	0.49

Trend analysis based on monthly rainfall gridded dataset

This research includes a month-based trend analysis of the study area. Figure 5 illustrates the collective rainfall distribution for individual months over 46 years. Figure 6a depicts the annual rainfall, with a minimum of 917.0 mm in 1976 and a maximum of 2352.9 mm in 2010. The annual average rainfall is lowest for November (5.72 mm), followed by December (18.24 mm), while it is highest for August (428.4 mm), followed by July (425.2 mm). Figure 6b showcases the monsoonal time series, with a minimum rainfall of 187.25 mm in 1987 and a maximum of 677.86 mm in 2010. Similarly, Fig. 6c illustrates the post-monsoonal time series, with a minimum rainfall of 0.4 mm in 1994 and a maximum of 89.05 mm in 1985. Furthermore, Fig. 6d displays the summer rainfall pattern, with a minimum of 19.50 mm in 1974 and a maximum of 183.68 mm in 2013, while Fig. 6e indicates the winter rainfall pattern, with a minimum of 12.84 mm in 2009 and a maximum of 106.49 mm in 2013.

Statistical characteristics of month-based trend analysis and variability pattern of rainfall dataset

The mean monthly rainfall of August ($M = 428.42$, $SD = 115.56$) is statistically higher whereas November ($M = 5.72$, $SD = 12.21$) records the least contribution of rainfall (Table 5). These results highlight the dominance of the monsoon season in the watershed, alongside noticeable effects from the post-monsoon season and sluggish rainfall

Fig. 4 Sen's slope values for annual and seasonal rainfall

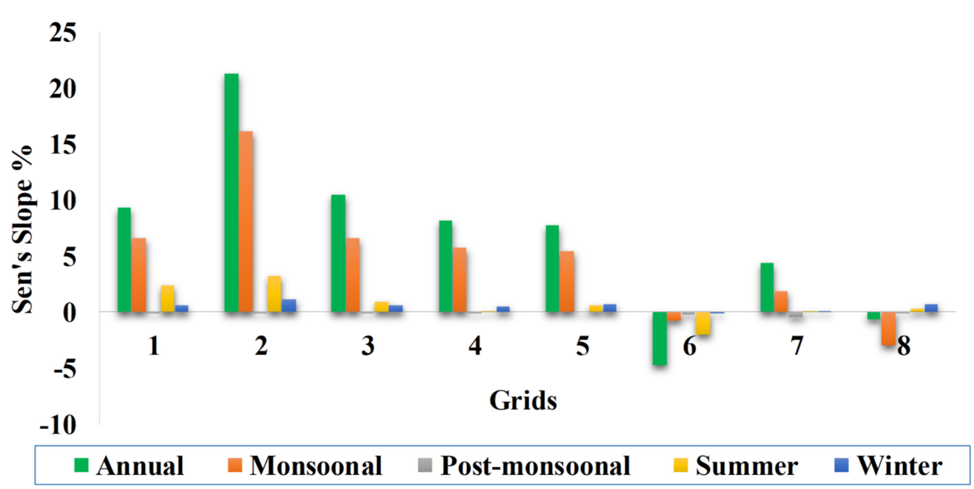

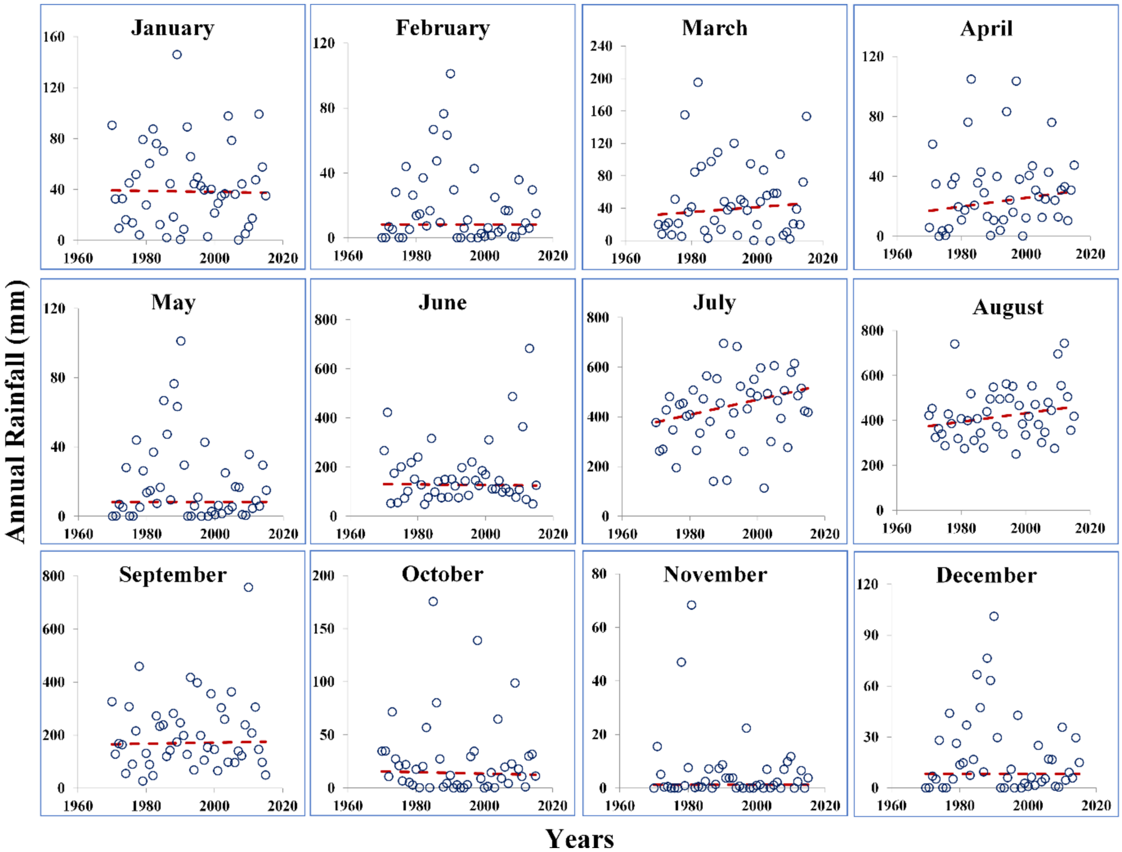

Fig. 5 Distribution of monthly-annual rainfall trend

patterns. It's observed that regions with inadequate rainfall also exhibit higher variability, significantly impacting agricultural and economic sectors, with water scarcity emerging as a chronic issue in areas with pronounced variability.

The Coefficient of Variation (CV), presented in Table 5, quantitatively measures the deviation of specific data points from their mean values. For mean annual rainfall in the study area, the CV ranges from 26.97 to 213.47% for August and November, with a weighted average of 91.02%. Remarkably, October, November, and December exhibit the highest variability, contributing the least to the overall rainfall percentage, standing at 1.72, 0.38, and 1.22%, respectively. These findings suggest that these months are comparatively the driest in the study area.

Analysis of *Zc*-Statistics of monthly rainfall trends

In the Mann–Kendall test, the rainfall trend has been calculated for each month individually along with Sen's magnitude of slope (Q). Table 6 exhibits *Zc*-statistic along with Sen's Slope values and explains that January, June and October show insignificantly negative trends, while the remaining months show positive trends. Specifically, February and July show positive trends with a significance level of 10 and 5%, respectively. Figures 7 and 8 closely align with Table 6, depicting a similar representation of trends, *Zc*-statistics and Sen's slope values.

Rainfall anomaly index (RAI)

'*RAI*' is used to interpret the intensity and frequency of wet and dry years. In this study, the annual '*RAI*' has been calculated on a monthly and yearly basis. The monthly '*RAI*' is evaluated for a particular year of the maximum anomaly. Van Rooy (1965) was the first to coin the term '*RAI*', which was further adopted by Freitas (1998). The Eqs. (8) and (9) of RAI include:

$$RAI = 3\left[\frac{N - \overline{N}}{\overline{M} - \overline{N}}\right], \quad \textit{for positive anomalies} \tag{8}$$

$$RAI = 3\left[\frac{N - \overline{N}}{\overline{X} - \overline{N}}\right], \quad \textit{for negative anomaly} \tag{9}$$

where N monthly or annual rainfall in mm; $\overline{N}$ monthly or annual average rainfall in mm; $\overline{M}$ average of the ten highest

Fig. 6 **a** Distribution of mean annual rainfall trend. **b** Distribution of monsoon rainfall trend. **c** Distribution of post-monsoonal rainfall trend. **d** Distribution of summer rainfall trend. **e** Distribution of winter rainfall trend

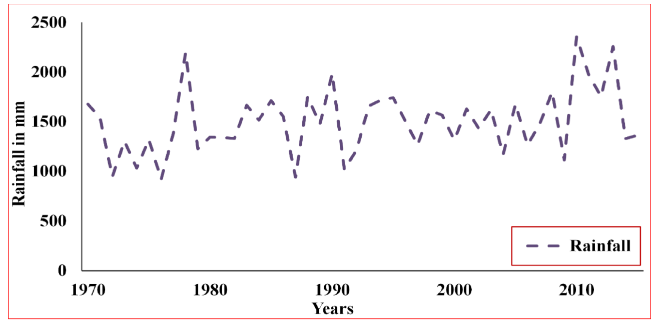

(a): Distribution of mean annual rainfall trend

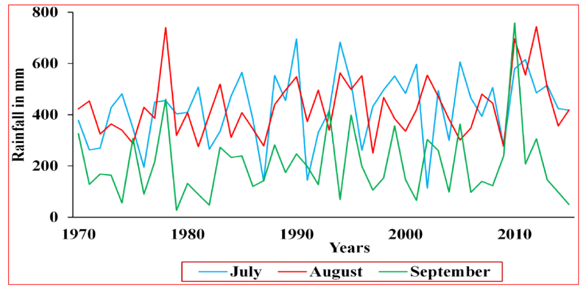

(b): Distribution of monsoon rainfall trend

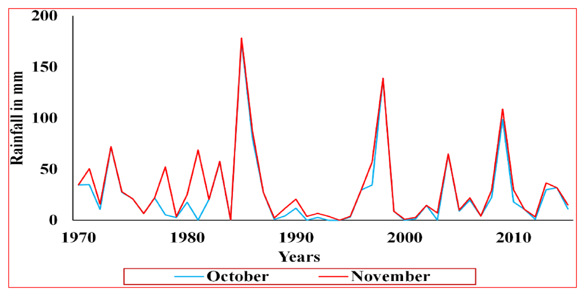

(c): Distribution of post-monsoonal rainfall trend

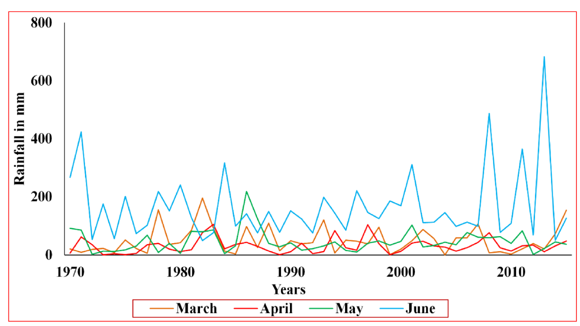

(d): Distribution of summer rainfall trend

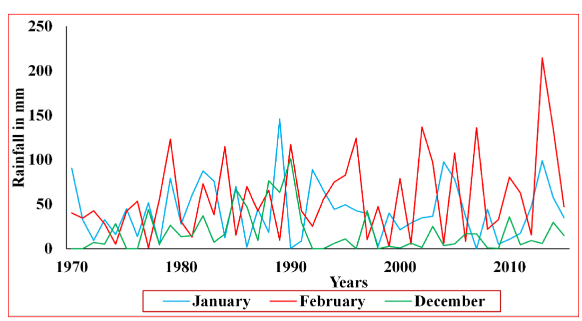

(e): Distribution of winter rainfall trend

Table 5 Statistical parameters related to monthly-annual trend analysis

Months	Minimum	Maximum	Mean	%	SD	CV (%)	Median
Jan	0.14	145.85	42.45	2.83	31.94	75.24	38.03
Feb	1.02	214.5	57.97	3.87	46.35	79.94	44.96
Mar	0.02	195.36	49.25	3.29	45.29	91.96	38.46
Apr	0	104.87	30.18	2.01	25.49	84.47	25.61
May	1.33	218.23	46.29	3.09	38.59	83.37	39.14
Jun	48.85	682.70	166.27	11.09	123.32	74.17	127.01
Jul	113.28	695.68	425.22	28.37	136.02	31.99	440.79
Aug	250.29	743.63	428.42	28.58	115.56	26.97	413.51
Sep	27.07	757.73	203.23	13.56	134.27	66.07	166.22
Oct	0	175.58	25.84	1.72	36.1	139.73	13.21
Nov	0	68.37	5.72	0.38	12.21	213.47	1.22
Dec	0	101.16	18.24	1.22	22.76	124.8	8.26

Table 6 Estimated *Zc*-statistic and Sen's slope values related to monthly-annual trends

Months	*Zc*-statistics	Trend	Sen slope
Jan	− 0.13	Decreasing	− 0.04
Feb	**1.67**[a]	Increasing	0.77
Mar	0.66	Increasing	0.3
Apr	1.33	Increasing	0.29
May	0.97	Increasing	0.33
Jun	− 0.21	Decreasing	− 0.12
Jul	**2.10**[b]	Increasing	3.02
Aug	1.57	Increasing	1.92
Sept	0.11	Increasing	0.21
Oct	− 0.54	Decreasing	− 0.07
Nov	0.28	Increasing	0
Dec	0.08	Increasing	0

Numbers in bold indicate significant values

[a]Significant at the 10% level

[b]Significant at the 5% level

monthly or annual rainfall in mm; $\overline{X}$ average of the ten lowest monthly or annual rainfall in mm;

Anomalies with values above average are referred to as positive (+) anomalies, while negative anomalies with values below average are referred to as negative (−) anomalies. Table 7 outlines the categorization of RAI (Rainfall Anomaly Index) ranges alongside the corresponding climate types associated with each range. The dry and wet years from 1975 to 2015 are visualised in this chapter using RAI (Fig. 9), which allows for the identification of years where these events are more intense and/or lasting.

Figure 9 represents dry and wet years. The negative values depict dry years whereas the positive value represents wet years with varying degrees of intensity. According to the classification given by Freitas (1998), the time series of 23 years with negative RAI varies between dry to very dry while the time series for the remaining 23 years with positive RAI varies between extreme wet to humid climatic

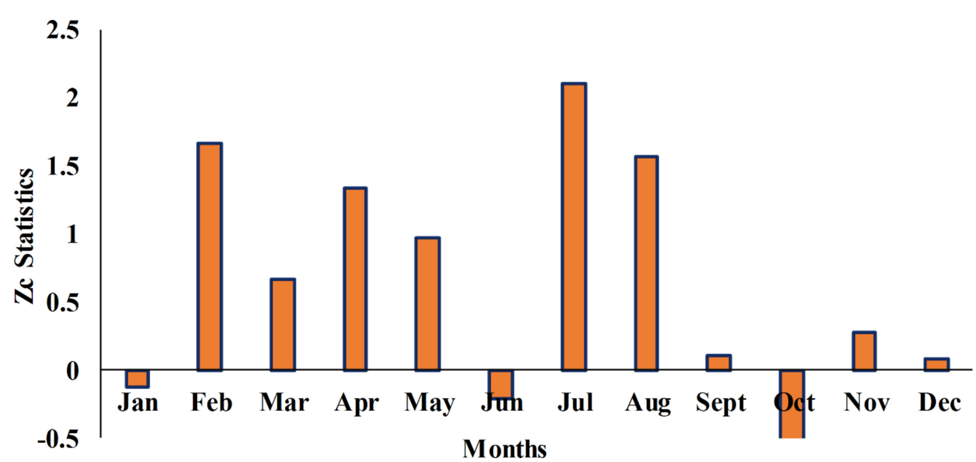

Fig. 7 Month-wise trend distribution of Zc-statistics

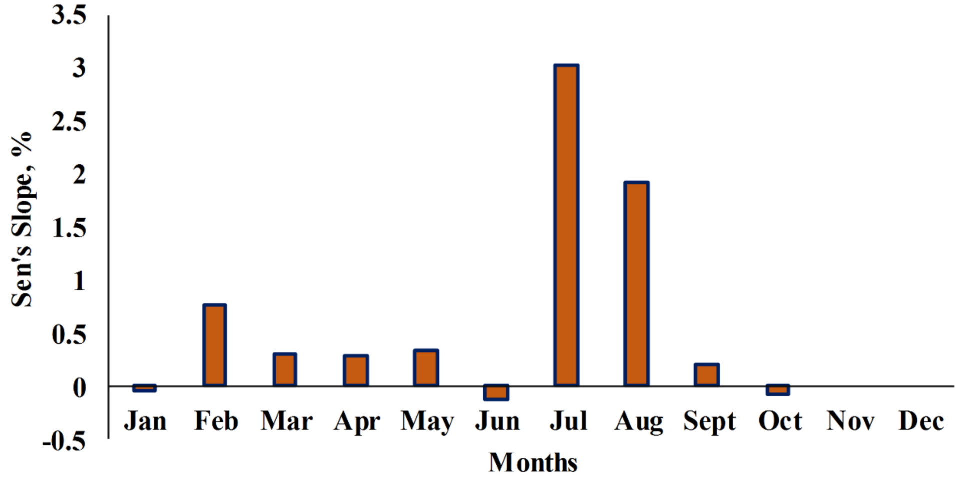

Fig. 8 Month-wise trend distribution of Sen's slope values

Table 7 Classification of rainfall anomaly index (RAI) intensity

	RAI range	Classification
Rainfall anomaly index (RAI)	Above 4	Extremely humid
	2–4	Very humid
	0–2	Humid
	− 2 to 0	Dry
	− 4 to − 2	Very dry
	Below-4	Extremely dry

Source: Freitas (1998)

conditions (Table 7). On the contrary, there is a representation of similar years of dry and rainy ones.

The time series that remained the longest with dry weather is from 1972 to 1977 and from 1979 to 1982 (Fig. 9). 1987 is the year having the highest negative value followed by 1976, with an RAI of − 1.60 and − 1.66 respectively, classified as dry. The period that remained the longest with rainy weather was from 1983 to 1986, from 1993 to 1996, and from 2010 to 2013. The year of high positive value was 2010 followed by 2013, with an average RAI of 1.31 and 1.17 respectively, being therefore classified as humid. Concerning the occurrence of dry and wet years, it is suggested that the depletion in the period between consecutive dry years dispersed by wet years favours the water supply to the watershed. A similar case was observed in the interval from 1979 to 1990 and 1993 to 2010.

Continuing this study, we further investigate the years exhibiting the most extreme anomalies in rainfall distribution across the area. Specifically, we analyse the monthly Rainfall Anomaly Index (RAI) values for the top two driest years, 1976 and 1987, as well as the wettest years, 2010 and 2013 (Fig. 9).

In Fig. 10, both the years, 2010 and 2013 represented an exact distribution of rainfall throughout the year, except February, June and September where the months show the appropriate difference in positive and negative RAI. The month of September receives the highest rainfall in the year 2010 whereas, in 2013, the month of June receives the maximum rainfall.

The driest years in the dataset (Fig. 11) represented above-average rainfall for July, August, and September. The month of May also represented RAI as rainy, but only for

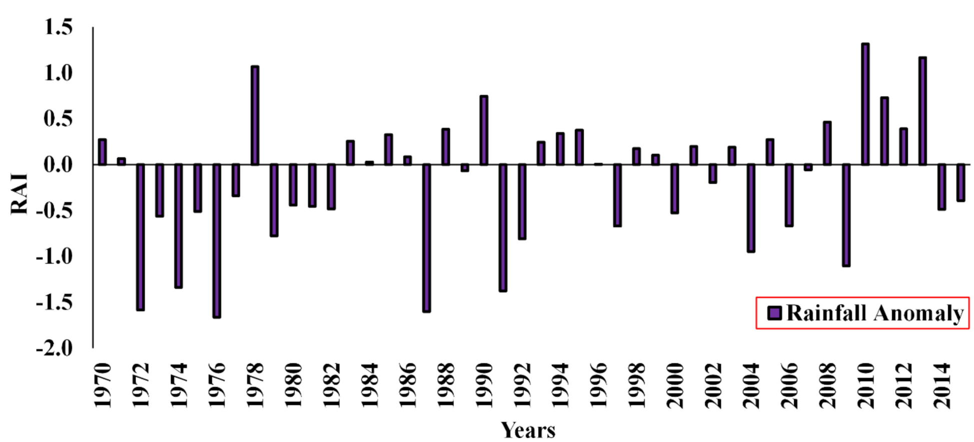

Fig. 9 Representation of rainfall anomalies in the area

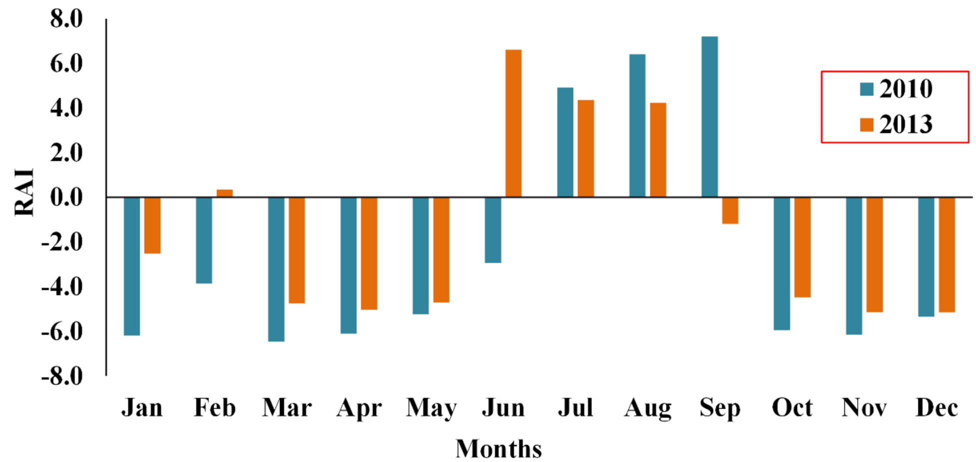

Fig. 10 Monthly Rainfall Anomaly Index (RAI) for rainy years

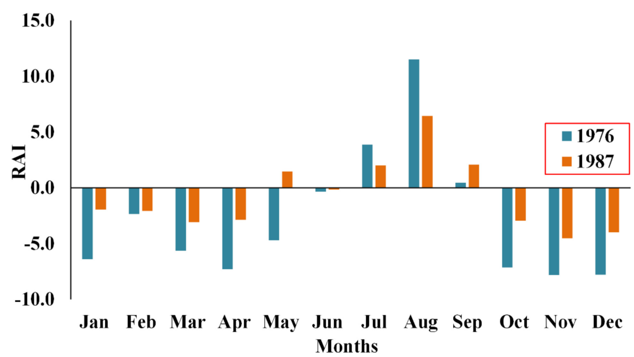

Fig. 11 Monthly Rainfall Anomaly Index (RAI) for dry years

the year 1976. In this context, it is observed that in very dry years, even in the rainy season, there are months when RAI tend to be negative. The months of November and December were the driest in 1976 and 1987, respectively.

Temperature trend analysis

Global climate change is directly proportional to the rise in temperature. In the present study, the monthly and annual status of the temperature dataset based on the trend and variability analysis is taken up. The temperature dataset for the last 39 years i.e. 1975–2013 is acquired from the Indian Meteorological Department (IMD). To achieve the objective, the linear regression method is used to analyse the behaviour of annual temperature. Table 8 summarises the characteristics of the minimum, maximum and mean temperature

Table 8 Statistical parameter related to temperature trend analysis

Months	Mean	Zc	β	Tmax	Zc	β	Tmin	Zc	B
Jan	12.04	− 1.35	− 0.017	18.12	**− 2.23**[a]	− 0.040	5.95	0.02	0.000
Feb	14.53	**2.25**[a]	0.037	20.95	1.40	0.027	8.12	**3.34**[b]	0.052
Mar	19.33	**3.19**[b]	0.065	26.30	**2.88**[b]	0.076	12.37	**3.92**[b]	0.063
Apr	25.00	**2.01**[a]	0.040	32.53	**1.84**[c]	0.032	17.46	**2.27**[a]	0.042
May	28.34	0.85	0.018	35.31	0.22	0.011	21.38	1.60	0.032
June	28.90	0.00	0.001	34.52	− 0.63	− 0.019	23.28	1.26	0.014
Jul	27.32	**2.64**[b]	0.029	31.28	1.35	0.020	23.37	**3.46**[b]	0.036
Aug	26.69	**2.37**[a]	0.015	30.41	0.75	0.006	22.97	**3.75**[b]	0.025
Sept	52.75	**1.74**[c]	0.016	30.24	− 0.24	− 0.005	21.27	**3.10**[b]	0.027
Oct	22.83	0.70	0.007	29.20	− 0.90	− 0.011	16.46	**1.67**[c]	0.024
Nov	18.17	0.92	0.012	25.22	− 0.65	− 0.006	11.11	**2.01**[a]	0.028
Dec	13.89	0.12	0.001	20.66	**− 1.98**[a]	− 0.019	7.12	**2.18**[a]	0.029

Number in bold indicate significant values

[a]Significant at the 5% level

[b]Significant at the 1% level

[c]Significant at the 10% level

of the study area based on the daily time series dataset. In addition to trend and variability analysis, we utilized the anomaly index to identify the coldest and warmest phases. In our analysis, temperature and time serve as dependent and independent variables, respectively, which are specified in Eq. 10:

$$\textbf{Temperature} = \textbf{t}\,(\textbf{time}) \quad \textbf{and} \quad \textbf{Y} = (\boldsymbol{\alpha} + \boldsymbol{\beta}\textbf{X} + \boldsymbol{\mu}) \tag{10}$$

where Y = mean temperature; X = known time, α = y-intercept, β = slope and μ = error/normally distributed random variable. The t-value of each parameter is calculated to check the statistical significance that null hypothesis β = 0. The student's t-statistics (Box 1981) is measured using Eq. (11):

$$t_{cal} = \frac{\hat{\beta}}{S.E.(\hat{\beta})} \tag{11}$$

where β is the coefficient (i.e., slope) and S.E. is the standard error of β which shows the rate of change in temperature per unit of time [Eq. (12)]. It is calculated as:

$$S_{yx} = \sqrt{\frac{\sum(y-\bar{y})^2 \frac{[\sum(x-\bar{x})(y-\bar{y})]^2}{\sum(x-\bar{x})^2}}{n-2}} \tag{12}$$

where n is the size of the sample.

Month-based temperature trend analysis:

Table 8 summarises the characteristics of the minimum, maximum and mean temperature of the study area based on the gridded dataset. The mean temperature of the study area varies from 12.04 °C (minimum) for January to 28.90 °C (maximum) for June with an annual average temperature of 21.90 °C.

Table 4 also demonstrated that the MK-test which revealed that minimum, maximum and mean temperature has been increasing through time significantly. The *Zc*-statistics value reveals that the mean temperature has an increasing trend through time except for January, which shows an insignificantly negative trend. The month of June also shows no variation in the trend. The months of February, April and August show a significantly increasing trend through time with 5% of the significance level. The months of March and July show an increasing trend of a 1% significance level and the month of September shows a significant increasing trend with a 1% significance level. The *Zc*-statistics value of maximum temperature revealed that June, September, October and November show insignificant negative trends while January and December show a significantly negative trend with a 5% level of significance. The months of March and April show a significantly positive trend with a 1% and 10% significance level. The *Zc*-statistics of minimum average temperature revealed a significant positive trend. The month of October shows a 10% significant level. The months of November, December and April show a 5% level of significance and the months of February, March, July, August, and September show a 1% level of significance. The months of January, May and June show an insignificant positive trend. The overall increase in the annual temperature observed in the study area is attributed to an increase in the minimum temperature (the increment of the minimum temperature is more pronounced than the maximum) (Asfaw et al. 2018). The month-based representation of the long-term temperature trend for the last 39 years (1975–2013) is shown in Fig. 12a–c.

Trend analysis of minimum temperature on an annual scale

The long-term minimum temperature in the study area is determined to be 15.90 °C. The annual minimum temperature varies from 14.84 °C in 1983 to 16.82 °C in 2004. The warmest year during the study period is 2004 when it is found to be 1.03 °C warmer than that of normal whereas the coldest year is observed to be 1983 which shows a fall of − 0.92 °C below the normal. The rate of change is defined by the slope of the regression line (linear regression model), which is for the present case 0.031 °C per decade shown in Fig. 13a.

Trend analysis of maximum temperature on an annual scale

The maximum annual temperature trends with regression are shown in Fig. 13b. The long-term annual maximum temperature for the study area is found to be 27.89 °C. The warmest year with a maximum temperature of 29.16 °C is 1987 which is 1.27 °C warmer than that of the normal. The coldest year is found to be 1997 with the annual maximum temperature of 26.35 °C, with a drop of − 1.54 °C below the normal. The linear trend in annual maximum temperature from 1975 to 2013 in the study area indicates an increasing trend of 0.0069 °C per decade. The rise in annual maximum temperature observed in the study area is in good agreement with the discoveries of other urban studies on climate change in the Himalayas (Bhutiyani et al. 2007, 2010). Different anthropogenic activities like human invasion of forests, construction of concrete structures, deforestation, rising CO_2 levels etc., are responsible for the rise in temperature particularly in the Himalayan region.

Trend analysis of mean temperature on an annual scale

The observed annual mean temperature is affected by minimum and maximum temperatures. The long-term annual mean temperature for the study area is evaluated to be 21.90 °C. As revealed from Fig. 13c annual mean

Fig. 12 **a** Monthly trends analysis for maximum temperature. **b** Monthly trends analysis for minimum temperature. **c** Monthly trends analysis for mean temperature

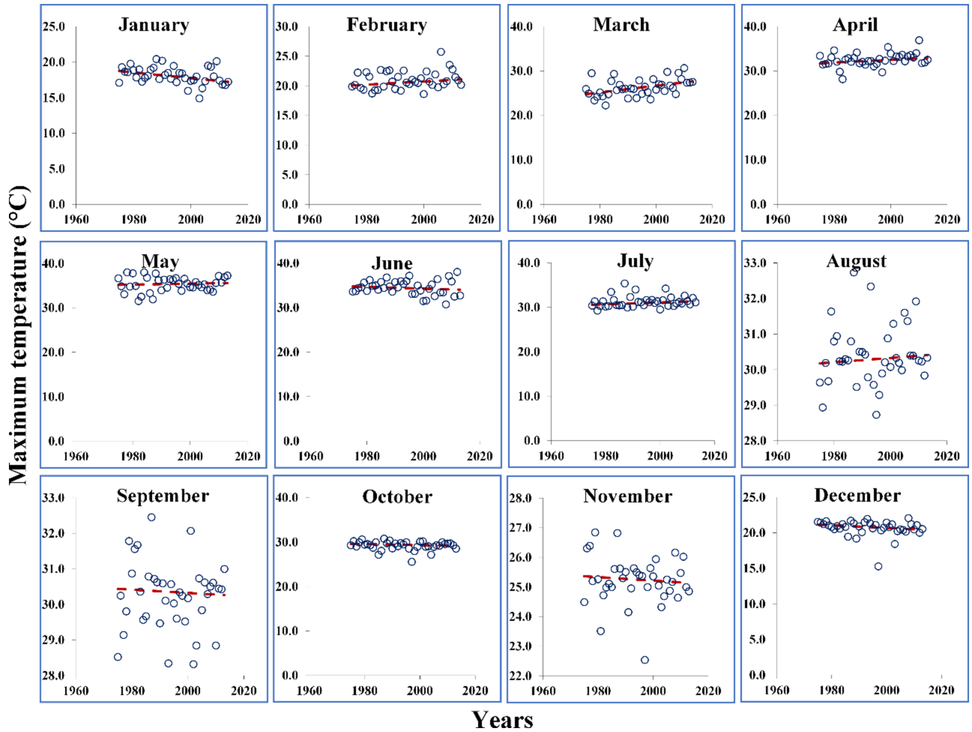

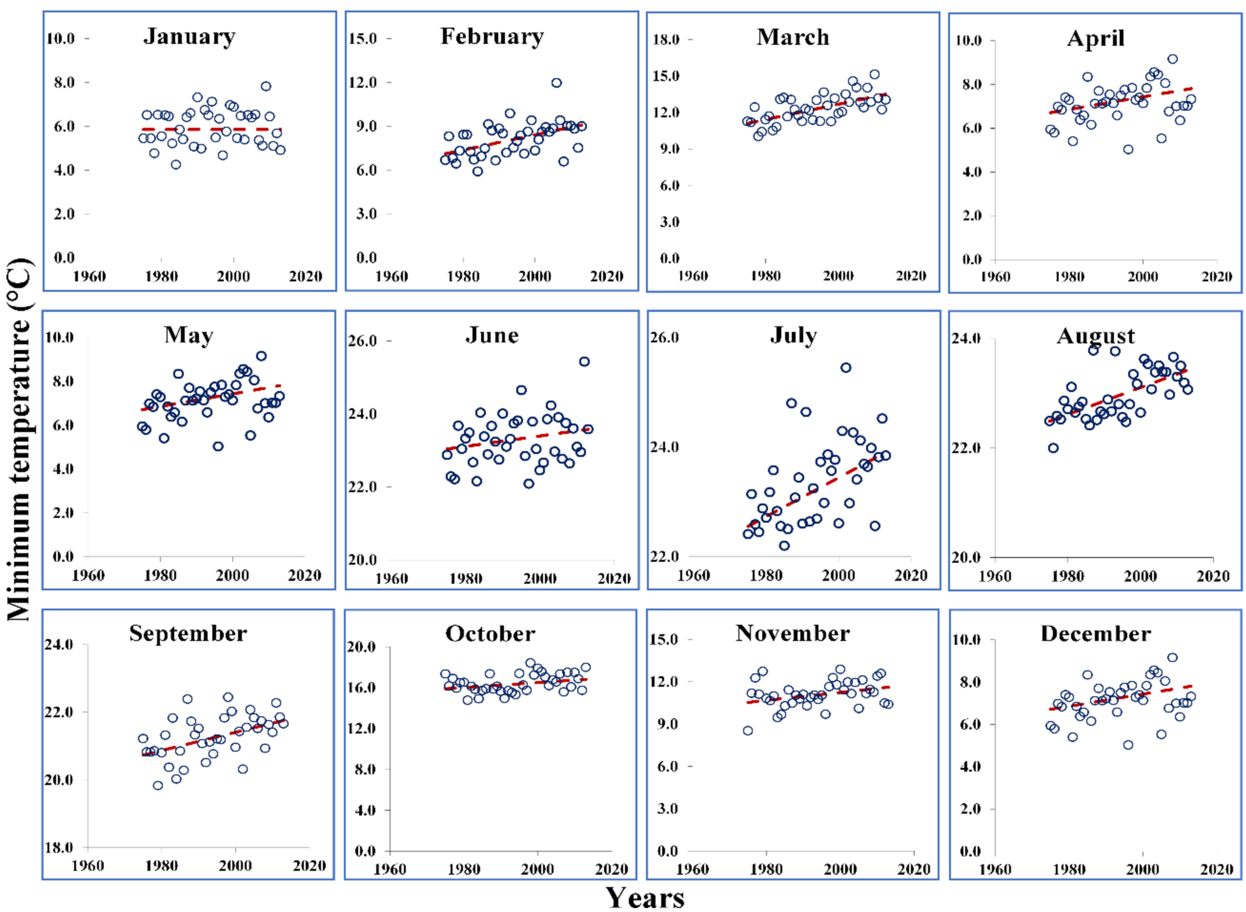

Fig. 12 (continued)

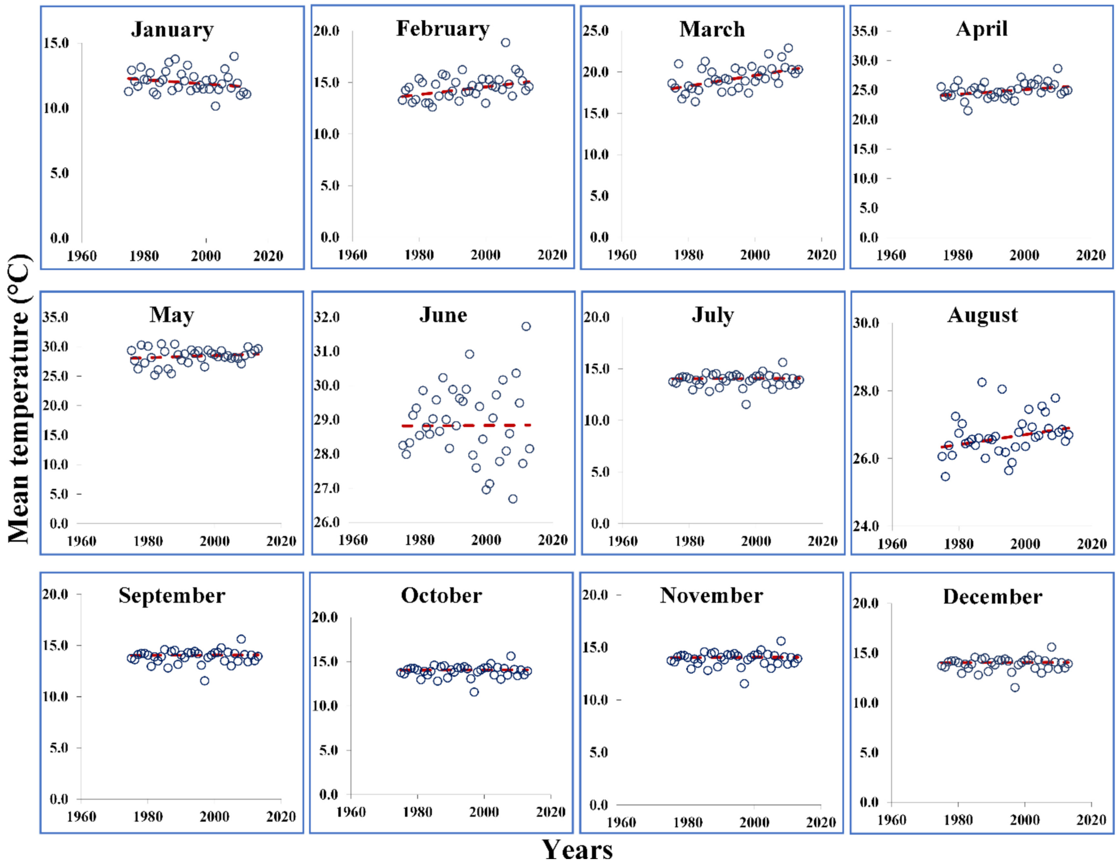

Fig. 12 (continued)

temperature witnessed a continuous period of warming since the year 2000 at Dehradun. After evaluation, it is found that the year 2010 is the warmest year with an annual mean temperature of 22.81 °C where the temperature rose by 0.91 °C more than normal. On the contrary, the year 1983 is considered as the coldest year with an annual mean temperature of 20.91 °C which is − 0.99 °C lower than that of the normal. The annual mean temperature trend with linear regression indicated an increasing trend of about 0.0193 °C per decade.

Temperature anomaly index (TAI)

Asfaw et al. (2018) defined temperature anomaly as "the difference between the actual temperature and the long-term average temperature"**.** A positive anomaly indicates that the temperature is warmer than the reference value or normal, while a negative anomaly indicates that the observed temperature is cooler than the reference value or normal. Evaluation of temperature anomalies for annual minimum, maximum and mean temperature is done for the study area for the time series of 1975–2013 and afterwards it is subtracted from the annual average minimum, maximum, and mean temperature. For analysing anomalies, the span of 30 years is considered an ideal period (Folland et al. 1999). In this study, the temperature anomaly is plotted against time and the observed linear trend is graphically represented. The value of linear trend, represented by the slope of a least-squares regression line with time as an independent variable indicates the magnitude of temperature rise or fall (Sundaresan et al. 2013).

Figure 14 reveals that the temperature anomaly of mean annual temperature expresses inter-annual variability whereas the trend after 1997 has been continuously higher till 2013. Negative anomalies are found to be more prominent during the initial years till 1997 while positive anomalies are prominent during the final ones. This phase can be attributed to the urbanization process in the watershed. The regression of annual mean temperature shows favourable positive trends and is demonstrated as statistically significant. The result is quite similar to the research of Stafford et al. (2000), Conway et al. (2004), Tabari and Talaee (2011), Roy and Das (2013) and Mengistu et al. (2014) which elaborate on the increasing trend in the minimum temperature series is higher than those in the maximum temperature series. Also, the trend of minimum, maximum and mean temperature has shown a statistically significant increasing trend.

Fig. 13 **a** Temperature pattern (Tmin) of the study area (1975–2013) with linear least squares regression lines. **b** Temperature pattern (Tmax) of the study area (1975–2013) with linear least square regression lines. **c** Temperature pattern (Tmean) of the study area (1975–2013) with linear least squares regression lines

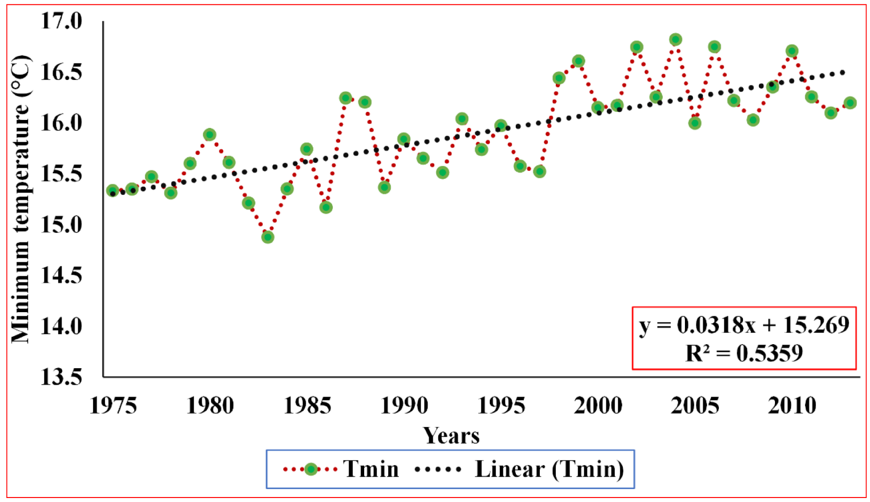

(a): Temperature pattern (Tmin) of the study area (1975-2013) with linear least squares regression lines.

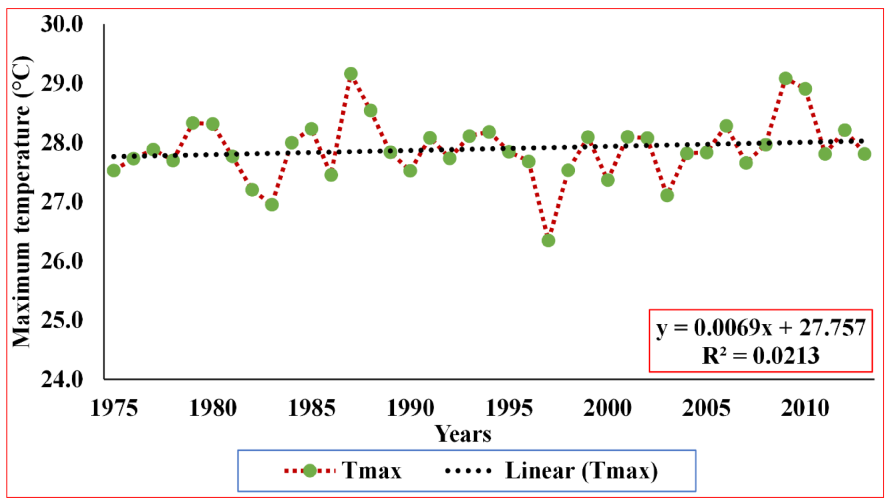

(b): Temperature pattern (Tmax) of the study area (1975-2013) with linear least square regression lines

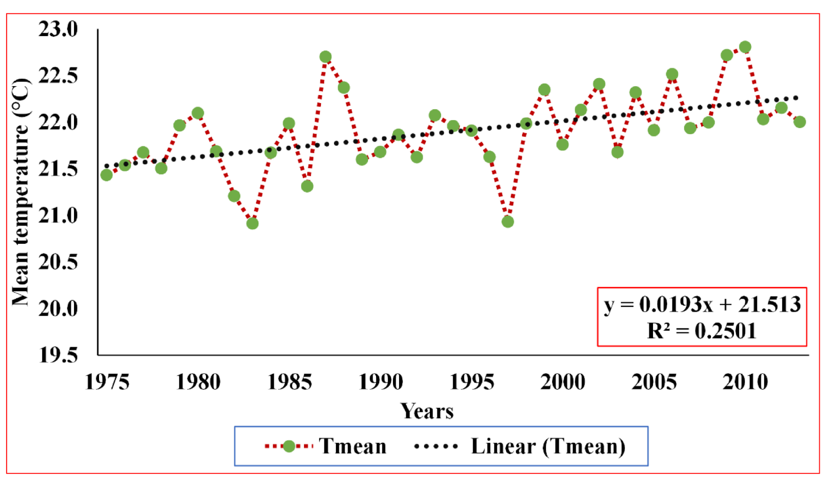

(c): Temperature pattern (Tmean) of the study area (1975-2013) with linear least squares regression lines.

Fig. 14 Temperature anomalies of the study area (1975–2013)

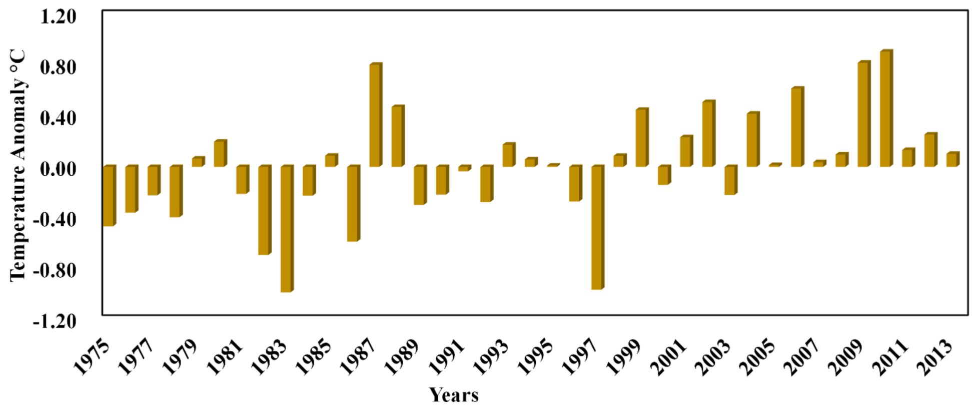

Conclusion

The present study has emphasized the potential effect of meteorological variables viz., rainfall and temperature regarding climate change is examined for trend detection and variability analysis.

Dehradun is one of the vulnerable cities in the Himalayan region concerning the context of urban climate change dominantly because of urbanization, industrialization and several anthropogenic activities. The recent study was conducted in the Asan River watershed and its surroundings situated in the Western Himalayas of Doon Valley, Uttarakhand, India. This study helps us to understand the changing climatic pattern over time with deterioration in rainfall and rising temperature. Rainfall data and temperature data for the last 46 (1970–2015) and 39 years (1975–2013) were purchased from IMD. Further, to achieve the opted objectives the trend analysis was estimated using the MK-test and Sen's slope estimators and further, the anomaly index was calculated. The overall study has been concluded with the mentioned points:

- Initially, the annual and seasonal rainfall revealed significant, however, varying trends in the grids. The monsoonal season, which occurs primarily in July, August and September, contributes most of the annual rainfall in the watershed. The study also found that after the monsoon season, the number of decreasing trends increases. Except for grid 6, which shows an insignificant decreasing trend (*Zc*-statistics) and slope for both the annual and seasonal rainfall, the *Zc*-statistics of the Mann–Kendall test reflect both positive and negative trends of rainfall in the area. Sen's slope estimator, which demonstrates a recurring change in the magnitude of the slope and the rainfall, also confirms a similar result. The Coefficient of Variance (CV) suggests that more rainfall in a particular grid corresponds to lesser variability. The overall analysis indicated a long-term increasing trend of annual rainfall in the watershed.
- Secondly, the month-based analysis concludes that July and August receive maximum rainfall whereas October, November and December contribute less percentage of rainfall and the highest value of variability.
- Thirdly, the analysis of rainfall anomaly reveals that the dataset presented a similar number of 23 years of rainy as well as the dry season. The months of November and December in 1987 are considered as driest and September in 2010 is considered as the wettest month in the year. The dry years present a positive anomaly in the months of the rainy season at the watershed.
- The MK-test trend analysis of annual temperature reveals that minimum, maximum and mean temperatures have been increasing over time. Additionally, the increase in minimum temperature is notably more pronounced than the rise in maximum temperature. The mean temperature in the study area is calculated to be 21.90 °C. Upon evaluation, it's observed that the warmest year was 2010, with an annual mean temperature of 22.81 °C, representing a rise of 0.91 °C compared to the normal. Conversely, the coolest year was 1983, with an annual mean temperature of 20.91 °C, indicating a temperature decrease of 0.99 °C compared to the normal. The rate of change of temperature is determined to be 0.031 °C, 0.0069 °C, and 0.0193 °C per decade for minimum, maximum, and mean temperatures, respectively, from 1975 to 2013.
- The analysis of temperature anomaly reveals that the dataset presented a mean annual temperature, which expresses inter-annual variability, while the trend after 1997 has been continuously increasing till 2013. Negative anomalies are much more pronounced in the initial years while positive anomalies are in the final. The regression of the annual mean temperature shows favourable positive trends and is demonstrated with statistical significance. This phase of temperature anomaly represented or attributed to the urbanization process in the watershed.

From all the statistical conclusions, it is evident that a significant change in rainfall trends has been observed over the past 46 years. The scrutiny and findings related to rainfall data can be valuable for managing water resources in the region. Based on previous research, it is speculated that recent urbanization and industrialization processes have contributed to these changes. The analysis of rainfall and temperature data supports the notion that variations in these factors are influenced by such activities, leading to shifts in the hydrological cycle and impacting agricultural productivity in the region and surroundings.

Funding The authors received no specific funding or research grant for this work from any agency in the public, commercial, or not-for-profit sectors, that could have influenced its outcome.

Declarations

Conflict of interest I testify on behalf of all co-authors that our research article submitted to 'Proceedings of the Indian National Science Academy' entitled 'Characterizing Temporal Variability in Meteorological Parameters Patterns in the Asan River Watershed, Uttarakhand, India: Insights from Long-Term Data Analysis'. We confirm that the work is original and it is neither published elsewhere nor under review. There is no conflict of interest for this work. Please address all correspondence concerning this manuscript to me at ankita.geors@gmail.com. I declare that this research article is the original part of my research, has been written by me and it is neither published elsewhere nor under review. The experimental work is almost entirely my work; the collaborative contributions have been indicated clearly and acknowledged.

References

Ademe, D., Zaitchik, B.F., Tesfaye, K., Simane, B., Alemayehu, G., Adgo, E.: Climate trends and variability at adaptation scale: patterns and perceptions in an agricultural region of the Ethiopian Highlands. Weather Clim Extremes **29**, 100263 (2020)

Asfaw, A., Simane, B., Hassen, A., Bantider, A.: Variability and time series trend analysis of rainfall and temperature in northcentral Ethiopia: a case study in Woleka sub-basin. Weather Clim Extremes **19**, 29–41 (2018)

Ayoade, J.A. (1983). Introduction to Climatology for the Tropics (No Title), pp. 204–223. Wiley, New York

Bhutiyani, M.R., Kale, V.S., Pawar, N.J.: Long-term trends in maximum, minimum and mean annual air temperatures across the Northwestern Himalayas during the twentieth century. Clim. Change **85**(1), 159–177 (2007)

Bhutiyani, M.R., Kale, V.S., Pawar, N.J.: Climate change and the precipitation variations in the northwestern Himalaya: 1866–2006. Int. J. Climatol.: J. r. Meteorol. Soc. **30**, 535–548 (2010)

Birsan, M.V., Molnar, P., Burlando, P., Pfaundler, M.: Streamflow trends in Switzerland. J. Hydrol. **314**, 312–329 (2005a)

Birsan, M.V., Molnar, P., Burlando, P., Pfaundler, M.: Streamflow trends in Switzerland. J. Hydrol. **314**(1–4), 312–329 (2005b)

Box, J.F.: Gosset, fisher, and the t-distribution. Am. Stat. **35**, 61–66 (1981)

CCSP: Climate change impacts in the United States; highlights US National Climate Assessment. Global Climate Change Research Program (CCSP), US (2014)

Chauhan, M.: A perspective on watershed development in the Central Himalayan state of Uttarakhand, India. Int. J. Ecol. Environ. Sci. **36**(4), 253–269 (2010)

Conway, D., Mould, C., Bewket, W.: Over one century of rainfall and temperature observations in Addis Ababa, Ethiopia. Int. J. Climatol.: J. r. Meteorol. Soc. **24**, 77–91 (2004)

Degefu, M.A., Bewket, W.: Variability and trends in rainfall amount and extreme event indices in the Omo-Ghibe River Basin, Ethiopia. Reg. Environ. Change **14**, 799–810 (2014)

Folland, C.K., Miller, C., Bader, D., Crowe, M., Jones, P., Plummer, N., Scholefield, P.: Workshop on indices and indicators for climate extremes, Asheville, NC, USA, 3–6 June 1997 Breakout Group C: temperature indices for climate extremes. Clim. Change **42**, 31–43 (1999)

Freitas, M.: A decision support system for monitoring meteorological drought in semi-arid regions. Rev. Tecnol. **19**, 19–30 (1998)

Gajbhiye, S., Meshram, C., Mirabbasi, R., Sharma, S.K.: Trend analysis of rainfall time series for Sindh river basin in India. Theoret. Appl. Climatol. **125**, 593–608 (2016a)

Gajbhiye, S., Meshram, C., Singh, S.K., Srivastava, P.K., Islam, T.: Precipitation trend analysis of Sindh River basin, India, from the 102-year record (1901–2002). Atmos. Sci. Lett. **17**, 71–77 (2016b)

Haan, C.T.: Statistical Methods in Hydrology. Iowa State University Press, Ames (1977)

Hamilton, J.P., Whitelaw, G.S., Fenech, A.: Mean annual temperature and total annual precipitation trends at Canadian biosphere reserves. Environ. Monit. Assess. **67**, 239–275 (2001)

Hare, W.: Assessment of knowledge on impacts of climate change–contribution. Arctic **100**(6), 25–35 (2003)

Jhajharia, D., Shrivastava, S.K., Sarkar, D.S., Sarkar, S.: Temporal characteristics of pan evaporation trends under the humid conditions of northeast India. Agric. for. Meteorol. **149**, 763–770 (2009)

Jhajharia, D., Yadav, B.K., Maske, S., Chattopadhyay, S., Kar, A.K.: Identification of trends in rainfall, rainy days and 24-hour maximum rainfall over subtropical Assam in Northeast India. C.R. Geosci. **344**, 1–13 (2012)

Jhajharia, D., Dinpashoh, Y., Kahya, E., Choudhary, R.R., Singh, V.P.: Trends in temperature over the Godavari river basin in southern peninsular India. Int. J. Climatol. **34**, 1369–1384 (2014)

Jhajharia, D., Kumar, R., Dabral, P.P., Singh, V.P., Choudhary, R.R., Dinpashoh, Y.: Reference evapotranspiration under changing climate over the Thar Desert in India. Meteorol. Appl. **22**, 425–435 (2015)

Karl, T.R., Jones, P.D., Knight, R.W., Kukla, G., Plummer, N., Razuvayev, V., Peterson, T.C.: A new perspective on recent global warming: asymmetric trends of daily maximum and minimum temperature. Bull. Am. Meteor. Soc. **74**, 1007–1024 (1993)

Kendall, M.G.: Rank Correlation Methods, 4th edn. Griffin, London (1948)

Kiros, G., Shetty, A., Nandagiri, L.: Analysis of variability and trends in rainfall over northern Ethiopia. Arab. J. Geosci. **9**, 451 (2016)

Krishan, R., Chandrakar, A., Nikam, B.R., Khare, D. (2016). Analysis of trends in rainfall over a century in eastern Ganga Canal Command. HYDRO2016. CWPRS Pune, India

Kumar, V., Jain, S.K., Singh, Y.: Analysis of long-term rainfall trends in India. Hydrol Sci J-J Sci Hydrol **55**, 484–496 (2010)

Landsberg, H.: Global climatic trends. In: Julian, L., Simon, S., Khan, H. (eds.) The Resourceful Earth, pp. 272–303. Basic Backwell Publishers Ltd, New York (1984)

Longobardi, A., Villani, P.: Trend analysis of annual and seasonal rainfall time series in the Mediterranean area. Int. J. Climatol. **30**, 1538–1546 (2010)

Mann, H.B.: Nonparametric tests against trend. Econometr.: J. Econometr. Soc. **13**(3), 245–259 (1945)

Mengistu, D., Bewket, W., Lal, R.: Recent spatiotemporal temperature and rainfall variability and trends over the Upper Blue Nile River Basin, Ethiopia. Int. J. Climatol. **34**, 2278–2292 (2014)
Modarres, R., Silva, V.P.: Rainfall trends in arid and semi-arid regions of Iran. J. Arid Environ. **70**, 344–355 (2007)
Negi, G.C.: Hydrological research in the Indian Himalayan mountain; soil and water conservation. Curr. Sci. **3**(8), 974–980 (2002)
Pandey, R.P., Ramasastri, K.S.: Relationship between the common climatic parameters and average drought frequency. Hydrol. Process. **15**, 1019–1032 (2001)
Parry, M., Parry, M.L., Canziani, O., Palutikof, J., Van der Linden, P., Hanson, C., et al.: Climate change 2007-impacts, adaptation and vulnerability: working group II contribution to the fourth assessment report of the IPCC, vol. 4. Cambridge University Press (2007)
Rao, B.D.V., Srinivasulu, D., Ratna, S.B.: Climate change with special reference to India: present and future scenarios. In: Bahadur, B., Satyanarayana, B. (eds.) Proc. of AP Academy of Sciences, Hyderabad special issue on Climate Change, vol. 11, no. 4, pp. 230–239 (2007)
Roy, T.D., Das, K.K.: Temperature trends at four stations of Assam during the period 1981–2010. Int. J. Sci. Res. Publ. **3**, 1–3 (2013)
Salmi, T., Maatta, A., Anttila, P., Ruoho-Airola, T., Amnell, T.: Detecting trends of annual values of atmospheric pollutants by the Mann-Kendall test and Sen's slope estimates MAKESENS–The excel template application. Finish Meteorological Institute, Helsinki (2002)
Sen, P.K.: Estimates of the regression coefficient based on Kendall's tau. J. Am. Stat. Assoc. **63**, 1379–1389 (1968)
Sharma, A., Bagri, D.S (2020). "Monitoring of Urban Sprawl and Spatio-temporal variability of Landuse/Landcover change in Asan Watershed, Doon Valley, Uttarakhand, India" AGU Fall meeting-2020, https://doi.org/10.1002/essoar.10505204.1.
Sharma, A., Nikam, B.R., Bagri, D.S., Kumar, D. (2020). Trend analysis of annual and seasonal time series over the last 46 years in Asan watershed, Doon valley based on the gridded dataset, Earth Sci. India **13**(1), 8–19 (2020). https://doi.org/10.31870/ESI.13.1.2020.2. ISSN: 0974-8350
Sharma, A., Nikam, B.R., Bagri, D.S., Kumar, D.: Geo-environmental investigations in the Asan River Watershed of Doon Valley, Uttarakhand. Ph.D thesis submitted to HNB Garhwal University/IIRS-ISRO Dehradun (2021). https://shodhganga.inflibnet.ac.in:8443/jspui/handle/10603/401114
Sharma, A., Krishan, R., Nikam, B., Bagri, D.S.: Urbanization trends and challenges: a case study in the Asan Watershed of Uttarakhand on Urban growth patterns and sustainable land use planning: PREPRINT (Version 2) available at Research Square (2024). https://doi.org/10.21203/rs.3.rs-3660810/v2
Singh, O., Arya, P., Chaudhary, B.S.: On rising temperature trends at Dehradun in Doon valley of Uttarakhand, India. J. Earth Syst. Sci. **122**, 613–622 (2013)
Singh, B.R.: Global Warming: Impacts and Future Perspective. BoD–Books on Demand (2012)
Stafford, J.M., Wendler, G., Curtis, J.: Temperature and precipitation of Alaska: 50-year trend analysis. Theoret. Appl. Climatol. **67**, 33–44 (2000)
Sundaresan, J., Gupta, P., Santosh, K.M., Boojh, R.: Climate Change & Himalayan Informatics. Scientific Publishers (2013)
Tabari, H., Talaee, P.H.: Analysis of trends in temperature data in arid and semi-arid regions of Iran. Glob. Planet. Change **79**, 1–10 (2011)
Tabari, H., Taye, M.T., Willems, P.: Statistical assessment of precipitation trends in the upper Blue Nile River basin. Stoch. Env. Res. Risk Assess. **29**, 1751–1761 (2015)
Theil, H.: A rank-invariant method of linear and polynomial regression analysis, Part 3. Proc. k. Ned. Akad. Weinenschatpen A **53**, 1397–1412 (1950)
Tigga, A., Hema Malini, B.: Temperature trends in Ranchi City, Jharkhand. Punjab Geographer **7**, 20–31 (2011)
Turkes, M.: Spatial and temporal analysis of annual rainfall variations in Turkey. Int. J. Climatol.: J. r. Meteorol. Soc. **16**, 1057–1076 (1996)
UAPCC: Uttarakhand Action Plan on Climate Change (UAPCC), Disaster Mitigation and Management Center. Government of Uttarakhand (GoUK). Supported by the United Nations Development Programme (UNDP) (2014). http://www.forest.uk.gov.in/files/USAPCC/Uttarakhand_SAPCC.pdf
Van Rooy, M.P.: A rainfall anomaly index independent of time and space. NOTOS **14**, 43–48 (1965)
Yue, S., Wang, C.: The Mann-Kendall test modified by effective sample size to detect trends in serially correlated hydrological series. Water Resour. Manage **18**(3), 201–218 (2004)
Yue, S., Pilon, P., Cavadias, G.: Power of the Mann-Kendall and Spearman's rho tests for detecting monotonic trends in hydrological series. J. Hydrol. **259**, 254–271 (2002)